

Boundary criticality for the Gross-Neveu-Yukawa models

Huan Jiang and Shao-Kai Jian*

Department of Physics and Engineering Physics, Tulane University, New Orleans, Louisiana 70118, USA

(Dated: March 21, 2025)

We study the boundary criticality for the Gross-Neveu-Yukawa (GNY) models. Employing interacting Dirac fermions on a honeycomb lattice with armchair boundaries, we use mean-field theory to uncover rich boundary criticalities at the quantum phase transition to a charge-density-wave (CDW) insulator, including the ordinary, special, and extraordinary transitions. The Dirac fermions satisfy a Dirichlet boundary condition, while the boson field, representing the CDW order, obeys Dirichlet and Neumann conditions at the ordinary and special transitions, respectively, thereby enriching the critical GNY model. We develop a perturbative $4 - \epsilon$ renormalization group approach to compute the boundary critical exponents. Our framework generalizes to other GNY universality class variants and provides theoretical predictions for experiments.

Introduction.— Boundary criticality captures the rich phenomenology of boundary effects in conformal field theory (CFT) [1]. It is well-known that the presence of boundaries enriches universality classes. For instance, in a free scalar field theory, there exist two distinct conformal boundary conditions, Dirichlet and Neumann, each leading to different boundary scaling dimensions for the scalar field. The situation becomes more intriguing in interacting theories, such as the interacting scalar CFT with $O(N)$ symmetry [2–8], which gives rise to a much richer landscape of boundary critical phenomena, broadly categorized under boundary CFT (BCFT). BCFT has a wide range of applications across various fields of physics, from the Kondo effect in condensed matter systems [9, 10] to holographic dualities in quantum gravity [11–13]. Consequently, exploring new boundary criticalities holds great significance across multiple disciplines.

Gapless Dirac fermions, which emerge in numerous condensed matter systems, including graphene [14], the surfaces of topological insulators [15, 16], and topological semimetals [17, 18], can drive exotic quantum phase transitions. For instance, the Ising transition is enriched to the chiral Ising universality class in the presence of Dirac fermions [19, 20]. In these critical theories, the scalar field couples to Dirac fermions via a Yukawa interaction, providing a realization of the Gross-Neveu-Yukawa (GNY) model [21–24]. It has also generated extensive research interest in the context of BCFT [25–33]. In particular, previous works [34, 35] pioneered the study of boundary criticality in the GNY universality class, identifying distinct boundary transitions, special, ordinary, and extraordinary, when Dirac fermions couple to a scalar field. However, it remains unclear how this theory describes boundary criticality in condensed matter systems and other variations of the GNY universality class.

In this paper, we systematically address these two questions. We construct a lattice model that hosts interacting Dirac fermions and an Ising transition with an open boundary condition. Using variational mean-field theory, we demonstrate that the model exhibits a rich boundary criticalities, including the ordinary, special, and extraordinary transitions. To formulate an effective field theory describing these boundary criticalities, we identify that the Dirac fermion satisfies a Dirichlet boundary condition [36], while the scalar field obeys Dirichlet

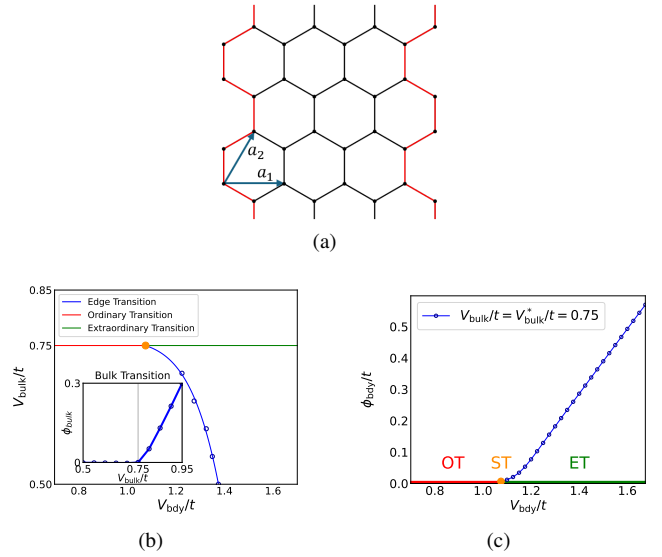


FIG. 1. (a) Illustration of the honeycomb lattice with armchair boundaries. The black (red) link denotes the bulk (boundary) bond. (b) Phase diagram of the lattice model (1). (c) Boundary order parameter as a function of the boundary interaction V_{bdy} strength at the bulk critical point V_{bulk}^* . OT, ST, and ET represent ordinary, special, and extraordinary transition, respectively.

and Neumann boundary conditions at the ordinary and special transitions, respectively. These conformal boundary conditions further enrich the critical GNY model. In particular, we develop a perturbative $4 - \epsilon$ renormalization group approach to compute the critical exponents. Our method is broadly applicable to other variants of the GNY universality class, including the chiral XY and chiral Heisenberg universality classes. Notably, our critical theory differs from previous works [34] that employed the AdS approach, which is attributed to the symmetry of the order parameters. As a result, we present, for the first time, the boundary critical exponents of the GNY universality class in the context of condensed matter theory, as summarized in Table I.

Lattice model.— We consider a system of spinless fermions on a honeycomb lattice with an armchair boundary condition

described by the Hamiltonian:

$$H = -t \sum_{\langle ij \rangle} (c_i^\dagger c_j + h.c.) + V_{\text{bulk}} \sum'_{\langle ij \rangle} \left(n_i - \frac{1}{2} \right) \left(n_j - \frac{1}{2} \right) + V_{\text{bdy}} \sum''_{\langle ij \rangle} \left(n_i - \frac{1}{2} \right) \left(n_j - \frac{1}{2} \right), \quad (1)$$

where c_i^\dagger (c_i) creates (annihilates) a fermion at site i , $\langle ij \rangle$ denotes a nearest neighbor bond connecting site i and j . The parameter t represents the hopping amplitude. The armchair boundaries of the honeycomb lattice are illustrated in Fig. 1, where the black and red links represent the bulk and boundary bonds, respectively. The parameters V_{bulk} and V_{bdy} are the interaction strengths at bulk and boundary bonds, respectively, with the summation, $\sum'_{\langle ij \rangle}$ and $\sum''_{\langle ij \rangle}$, covering bulk and boundary bonds accordingly.

Using mean field calculation, we obtain the phase diagram shown in Fig. 1 (b). As the bulk interaction strength V_{bulk} increases, the system undergoes a quantum phase transition at V_{bulk}^* from a Dirac semimetal to a charge density wave (CDW) insulator, characterized by the CDW order parameter,

$$\phi = \sum_i (-1)^{s(i)} n_i, \quad (2)$$

where $s(i) = 0, 1$ for two sublattices indicates the staggered density order. This quantum phase transition belongs to the chiral Ising universality class [37].

The boundary criticality characterizes the influence of the boundary at the quantum critical point $V_{\text{bulk}} = V_{\text{bulk}}^*$. As shown in Fig. 1 (c), the boundary order parameter $\hat{\phi}$, defined as the CDW order located at the boundary:

$$\hat{\phi} = \sum_i'' (-1)^{s(i)} n_i, \quad (3)$$

becomes nonzero when the boundary interaction strength V_{bdy} exceeds a critical value V_{bdy}^* . For $V_{\text{bdy}} < V_{\text{bdy}}^*$, the boundary order remains zero, corresponding to the ordinary transition. In contrast, when $V_{\text{bdy}} > V_{\text{bdy}}^*$, the boundary order acquires a finite value, marking the extraordinary transition. The special transition occurs precisely at $V_{\text{bdy}} = V_{\text{bdy}}^*$.

Field theory.— To investigate the BCFT of the lattice model, we derive its effective field theory. The Dirac Hamiltonian is given by $\mathcal{H} = k_x \tau^z \sigma^x + k_y \sigma^y$, where $k_{x,y}$ denotes the momentum operator and the Pauli matrices σ^i and τ^i characterizes the sublattice and valley degrees of freedom, respectively [14]. It is well-known that the bulk quantum phase transition falls within the chiral Ising universality class, described by the action:

$$S = \int_{\mathcal{M}} d^d x \left(\sum_j \bar{\psi}_j \gamma^\mu \partial_\mu \psi_j + \frac{1}{2} (\partial_\mu \phi)^2 + \frac{\lambda}{4!} \phi^4 - i g \sum_j \phi \bar{\psi}_j \gamma^5 \psi_j \right), \quad (4)$$

where ψ_j represents the Dirac fermion fields and ϕ is the order parameter field [38]. ∂_μ denotes derivatives regarding (imaginary) time $x_0 \equiv \tau$ and space $x_i, i = 1, \dots, d-1$. γ_μ are gamma matrices: $\gamma^0 = \tau^y \sigma^x$, $\gamma^1 = \tau^x$, $\gamma^2 = \tau^y \sigma^z$, $\gamma^3 = \tau^z$, and $\gamma^5 = \tau^y \sigma^y$, and $\bar{\psi} = \psi^\dagger \gamma^0$. This convention of gamma matrices is introduced in the Supplemental Material [39]. Note that, to make our theory more general, we extend the fermion sector to include N flavors, denoted as ψ_j for $j = 1, \dots, N$. The parameters λ and g represent the quartic boson self-interaction and the fermion-boson Yukawa coupling, respectively. The Yukawa coupling can be understood as follows: the CDW order corresponds to a staggered density between two sublattices, which is captured by $\sigma^z = -i\gamma^0\gamma^5$.

The integration domain of the action is the bulk region \mathcal{M} , with full theory supplemented by boundary conditions. We assume that the field theory is located in a d -dimensional semi-infinite spacetime, $\mathcal{M} = \{x_\mu | x_1 > 0\}$ where the boundary is $\partial\mathcal{M} = \{x_\mu | x_1 = 0\}$. For convenience, we denote the hyperspace parallel to the boundary as y and the coordinate perpendicular to the boundary as x . The boundary condition for the Dirac fermion arises from the vanishing of the lattice fermion outside the lattice sites, enforcing a Dirichlet boundary condition [40], and for completeness, we review its derivation in the Supplemental Material. In our convention, the boundary condition for the Dirac fermion field is $-\gamma^1 \psi|_{\text{bdy}} = \psi|_{\text{bdy}}$. For the boson field, the boundary condition can be implemented through a boundary mass term, given by $\int_{\partial\mathcal{M}} d^{d-1} x \frac{c}{2} \phi^2$, where c is the boundary mass. This is connected to the boundary transitions: when $c > 0$, the boundary order remains zero corresponding to the ordinary transition, while for $c < 0$, the boundary order becomes nonzero corresponding to the extraordinary transition, and $c = 0$ corresponds to the special transition occurs at [41].

The effect of these boundary conditions is reflected in the bare propagators for the fermion and boson fields, which are detailed in the Supplemental Material. Here, we summarize the key results for the bare propagators. Due to translation symmetry in the hyperspace parallel to the boundary, the propagator can be conveniently expressed in a mixed representation, using momentum k_μ (for $\mu \neq 1$) along the boundary and a real-space coordinate perpendicular to the boundary. The fermion propagator reads

$$G(k, x, x') = G_b(k, x, x') + G_s(k, x, x'), \quad (5)$$

$$G_b(k, x, x') = \left(\frac{i\mathcal{k}}{2q} - \frac{\gamma^1}{2} \text{sgn}(x - x') \right) e^{-q|x-x'|}, \quad (6)$$

$$G_s(k, x, x') = -\gamma^1 \left(\frac{i\mathcal{k}}{2q} + \frac{\gamma^1}{2} \right) e^{-q(x+x')}, \quad (7)$$

where $\mathcal{k} = \sum_{\mu \neq 1} k_\mu \gamma^\mu$ and $q^2 = \sum_{\mu \neq 1} k_\mu^2$. It is evident that G_b and G_s correspond to the contributions with and without translation symmetry, respectively. The presence of G_s arises due to the Dirichlet boundary condition.

On the other hand, in the presence of a boundary mass term,

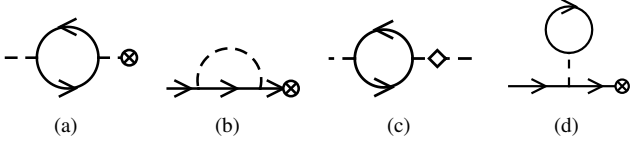


FIG. 2. Feynman diagrams relevant to the boundary field. The dashed (solid) line represents the boson (fermion) propagator. The vertex \otimes represents the boundary boson or fermion field and \diamond represents the boundary mass term.

the boson propagator is given by

$$D_c(k, x, x') = \frac{1}{2q} \left(e^{-q|x-x'|} + \frac{q-c}{q+c} e^{-q(x+x')} \right). \quad (8)$$

It is well-known that the limit $c \rightarrow \infty$ corresponds to the Dirichlet conformal boundary condition, while $c = 0$ corresponds to the Neumann boundary condition for the scalar boson [2–4]. Hence, the boson propagator can be simplified as

$$D(k, x, x') = D_b(k, x, x') + w D_s(k, x, x'), \quad (9)$$

$$D_b(k, x, x') = \frac{e^{-q|x-x'|}}{2q}, \quad D_s(k, x, x') = \frac{e^{-q(x+x')}}{2q} \quad (10)$$

The coefficient w distinguishes the boundary conditions, with $w = -1$ ($w = 1$) corresponding to the Dirichlet (Neumann) boundary condition.

Renormalization group.— The propagators in (5) and (9) serve as the building block for the RG analysis. In both G_s and D_s , the dependence on the coordinate perpendicular to the boundary is exponentially suppressed when either x or x' is deep in the bulk, i.e., $x, x' \gg 1$. This suppression indicates that boundary effects do not contribute to the bulk RG equations. Consequently, the bulk RG equations remain identical to those of the chiral Ising universality class. For completeness, we present the one-loop RG equations in the Supplemental Material and the fixed point, $\lambda^* = \frac{8\pi^2[(3-2N)+\sqrt{4N^2+132N+9}]}{3(2N+3)}\epsilon$, $g^* = \frac{2\pi\sqrt{\epsilon}}{\sqrt{3/2+N}}$, corresponding to the well-known chiral Ising universality class.

The presence of a boundary introduces new critical exponents for the boundary fields. In particular, the two leading boundary operators are the Dirac fermion $\hat{\psi} \equiv \psi(x=0)$ and the scalar boson at the boundary. Here, we use a hat to denote boundary fields. For the boundary scalar boson field, it is essential to distinguish between the Dirichlet and Neumann boundary conditions. Under the Dirichlet boundary condition, the field value is fixed to zero, $\hat{\phi} = 0$, making $\partial\hat{\phi} \equiv \partial_x\hat{\phi}$ the leading boundary scalar operator. In contrast, for the Neumann boundary condition, the leading boundary scalar field is $\hat{\phi}$ itself. Additionally, an extra relevant operator arises, corresponding to the boundary mass term $\hat{\phi}^2$ at the Neumann boundary condition.

We first examine the ordinary transition that corresponds to the Dirichlet boundary condition for the scalar field. The boundary critical exponent for a pure scalar theory has been

previously determined, so our focus here is on the additional contribution arising from the presence of Dirac fermions. We introduce the boundary RG factor $Z_{\partial\hat{\phi}}$ and $Z_{\hat{\psi}}$ for the fermion field and boson fields, respectively, as follows, $\partial\hat{\phi} = \sqrt{Z_{\phi}Z_{\partial\hat{\phi}}}\partial\hat{\phi}_R$, and $\psi = \sqrt{Z_{\psi}Z_{\hat{\psi}}}\hat{\psi}_R$. Here $Z_{\phi} = 1 - \frac{Ng^2}{4\pi^2\epsilon}$ and $Z_{\psi} = 1 - \frac{g^2}{16\pi^2\epsilon}$ (at the one-loop order) are the RG factors of the bulk chiral Ising class.

To proceed, we analyze the two-point function $\langle\phi\partial\hat{\phi}\rangle$. The Yukawa coupling generates a one-loop Feynman diagram for the boundary scalar field, illustrated in Fig. 2 (a), which takes the form:

$$\int dx_1 dx_2 D(p, x, x_1) G_2(p, x_1, x_2) [\partial_{x'} D(p, x_2, x')]_{x'=0} \quad (11)$$

where G_2 represents the fermion bubble, given by

$$G_2(p, x_1, x_2) = \int d^{d-1}y e^{-ip \cdot y} \times \text{Tr} [\gamma^5 G(y, x_1, x_2) \gamma^5 G(-y, x_2, x_1)]. \quad (12)$$

To interpret this expression, we start with a real-space representation, assigning the two vertices in Fig. 2 (a) to the coordinates (y, x_1) and $(0, x_2)$, respectively. We then treat the fermion bubble as an effective propagator rather than a closed loop and perform a Fourier transformation along the hyperspace direction to obtain the mixed representation. This precisely corresponds to the formulation in (12). After incorporating this fermion bubble, integrating over x_1 and x_2 leads to a singularity, as detailed in the Supplemental Material. The result can be summarized as:

$$\begin{aligned} &\langle\phi(p, x)\partial_x\phi(p', 0)\rangle \\ &= (2\pi)^{d-1}\delta(p+p')e^{-px} \left(1 + \frac{\lambda}{32\pi^2\epsilon} - \frac{Ng^2}{8\pi^2\epsilon} \right), \end{aligned} \quad (13)$$

where the Dirac delta function should be understood as component-wise. Inside the bracket, the first term corresponds to the tree-level contribution, the second term arises from boson self-interactions, and the third term represents the correction from the Yukawa coupling. From this, the RG factor for the boundary scalar field reads $Z_{\partial\hat{\phi}} = 1 + \frac{\lambda}{16\pi^2\epsilon} + \frac{Ng^2}{4\pi^2\epsilon}$.

Next, we analyze the two-point function $\langle\psi\hat{\psi}\rangle$ to determine the RG factor for the boundary fermion field. The corresponding Feynman diagram, illustrated in Fig. 2 (b), leads to the following expression:

$$\int dx_1 dx_2 G(p, x, x_1) \tilde{G}_2(p, x_1, x_2) G(p, x_2, 0), \quad (14)$$

where $\tilde{G}_2(p, x_1, x_2)$ is given by

$$\begin{aligned} &\tilde{G}_2(p, x_1, x_2) = \\ &= \int d^{d-1}y e^{-ip \cdot y} \gamma^5 G(y, x_1, x_2) \gamma^5 D(y, x_1, x_2). \end{aligned} \quad (15)$$

The reasoning behind this expression follows similarly from the analysis of the fermion bubble, and the RG procedure is

GNY	Ordinary transition		Special transition		
	$\Delta_{\hat{\psi}}$	$\Delta_{\partial\hat{\phi}}$	$\Delta_{\hat{\psi}}$	$\Delta_{\hat{\phi}}$	$\Delta_{\hat{\phi}^2}$
CI	$\frac{2}{3} - \frac{5+4N}{12+8N}\epsilon$	$2 - \frac{21+22N+\sqrt{4N^2+132N+9}}{12(3+2N)}\epsilon$	$\frac{3}{2} - \frac{3+4N}{12+8N}\epsilon$	$1 - \frac{21-2N+\sqrt{4N^2+132N+9}}{12(3+2N)}\epsilon$	$2 - \frac{15-4N-\sqrt{4N^2+312N+9}}{6(3+2N)}\epsilon$
CH	$\frac{3}{2} - \frac{8N-1}{4+16N}\epsilon$	$2 - \frac{3(9+52N)+5\sqrt{16N^2+344N+1}}{44(1+4N)}\epsilon$	$\frac{3}{2} - \frac{8N-7}{4+16N}\epsilon$	$1 - \frac{27-20N+5\sqrt{16N^2+344N+1}}{44(1+4N)}\epsilon$	$2 - \frac{17-24N-5\sqrt{16N^2+344N+1}}{22(1+4N)}\epsilon$

TABLE I. Boundary scaling dimensions for the GNY universality class, including the chiral Ising (CI) and the chiral Heisenberg (CH) universality class. $\epsilon = 4 - d$, and N denotes the flavor of four-component fermions in CI and eight-component fermions in CH.

also analogous. Therefore, we leave the detailed derivation to the Supplemental Material and present the result for the RG factor, $Z_{\hat{\psi}} = 1 - \frac{g^2}{16\pi^2\epsilon}$. With the RG factors, namely, the scaling dimension of the boundary fields at the ordinary transition can now be determined as $\Delta_{\partial\hat{\phi}} = \frac{d}{2} + \eta_{\partial\hat{\phi}}$ where $\eta_{\partial\hat{\phi}} = \frac{1}{2} \frac{d \log Z_{\partial\hat{\phi}}}{d \log \mu}$, and similarly for the Dirac fermions. The results are summarized in Table I.

Now, we turn to the discussion of the special transition, where the boson field satisfies the Neumann boundary condition. This scenario introduces several modifications, including changes in the leading boundary boson field and the boundary mass term. The leading boundary boson field is $\hat{\phi}$ instead of $\partial\hat{\phi}$. The inclusion of the boundary mass term is necessary because, at the special transition, the tree-level boundary mass parameter is $c = 0$, implying a relevant perturbation induced by the boundary mass term. To account for these effects, we introduce the RG factors for the boson field and the boundary mass term: $\hat{\phi} = \sqrt{Z_{\hat{\phi}} Z_{\hat{\phi}^2}} \hat{\phi}_R$ and $\hat{\phi}^2 = Z_{\hat{\phi}^2} \hat{\phi}_R^2$. The RG factor for the boundary fermion field remains the same as in the previous case.

The calculation of the RG factors for the leading boundary boson and fermion fields follows the same approach as in the ordinary transition. The results are summarized as $Z_{\hat{\phi}} = 1 + \frac{\lambda}{16\pi^2\epsilon} - \frac{Ng^2}{4\pi^2\epsilon}$ and $Z_{\hat{\psi}} = 1 - \frac{3g^2}{16\pi^2\epsilon}$. Next, we discuss the evaluation of the RG factor $Z_{\hat{\phi}^2}$. It can be obtained from the correlation function, $\langle \phi \phi \frac{1}{2} \hat{\phi}^2 \rangle$. The pure boson contribution is detailed in the Supplemental Material. Here, we focus on the one-loop diagram contributed from the Yukawa coupling, as shown in Fig. 2 (c):

$$\int dx_1 dx_2 D(p, x, 0) D(p', 0, x_1) G_2(p', x_1, x_2) D(p', x_2, x'),$$

where $G_2(p, x_1, x_2)$ is the fermion bubble given in (12). The divergence is evaluated in detail in the Supplemental Material, and summarized as

$$\begin{aligned} \langle \phi(p, x) \phi(p', x') \frac{1}{2} \phi^2(P, 0) \rangle = \\ (2\pi)^{d-1} \delta(P + p + p') \frac{e^{-p \cdot x - p' \cdot x'}}{pp'} \left(1 - \frac{\lambda}{16\pi^2\epsilon} - \frac{3Ng^2}{8\pi^2\epsilon} \right), \end{aligned} \quad (16)$$

where $\phi^2(P, 0) = \int d^{d-1} y e^{-iP \cdot y} \phi^2(y, 0)$. In the bracket, the first term corresponds to the tree-level contribution, the second term arises from boson self-interactions, and the third term represents the correction from the Yukawa coupling.

From this, we obtain the RG factor for the boundary mass term: $Z_{\hat{\phi}^2} = 1 - \frac{\lambda}{16\pi^2\epsilon} - \frac{3Ng^2}{8\pi^2\epsilon}$. With the RG factors, the scaling dimension of the boundary fields at the special transition are determined similarly as before, and summarized in Table I.

Other variants of GNY universality class.— Our methodology can be extended to other variants of the GNY universality class. The chiral Heisenberg universality class describes a quantum phase transition from a Dirac semimetal to an anti-ferromagnetic (AFM) insulator, where the order parameter is an $O(3)$ vector field that couples to the spin degrees of freedom of the Dirac semimetal [42, 43]. To formulate this transition, we present the field theory action:

$$\begin{aligned} S = \int_{\mathcal{M}} d^d x \left(\sum_j \bar{\psi}_j \gamma^\mu \partial_\mu \psi_j + \frac{1}{2} \sum_{i=1,2,3} (\partial \phi_i)^2 \right. \\ \left. + \frac{\lambda}{4!} \left(\sum_{i=1,2,3} \phi_i^2 \right)^2 - ig \sum_{i=1,2,3} \sum_j \phi_i \bar{\psi}_j \gamma^5 s^i \psi_j \right) \quad (17) \end{aligned}$$

where ψ_j and ϕ_i denote the Dirac fermion and the vector boson fields, respectively. The parameters λ and g represent the boson self-interaction and the Yukawa coupling, respectively. The gamma matrices satisfy $\{\gamma^\mu, \gamma^\nu\} = 2\delta^{\mu\nu}$ while s^i are the Pauli matrices representing the spin degrees of freedom [44]. Notably, the inclusion of spin degrees of freedom results in an eight-component Dirac fermion. Furthermore, as before, we generalize the Dirac fermion to have N flavors.

The boundary condition for the Dirac fermion fields remains the same, $-\gamma^1 \psi|_{\text{bdy}} = \psi|_{\text{bdy}}$. This boundary condition can still be derived from a honeycomb lattice model with armchair boundaries. More importantly, because the $SU(2)$ spin rotation symmetry is independent of the presence of open boundaries, the boundary condition for the vector boson fields must also be compatible with spin rotation symmetry. As the result, the propagator for the vector boson fields takes the form $D_{ij}(k, x, x') = \delta_{ij} D(k, x, x')$, where $D(k, x, x')$ is given in (9). With these propagators, the RG analysis follows the same procedure as in the chiral Ising universality class, and the final results are summarized in Table I.

Finally, we discuss the role of the symmetry in the presence of open boundaries and the chiral XY universality class, which arises in the Kekulé valence-bond-solid transition in a 2D Dirac semimetal [45]. In previous cases, the presence of open boundaries does not affect the symmetry under consideration. In the case of the chiral Ising transition, the CDW breaks a

reflection symmetry that interchanges two sublattices. This reflection symmetry is intact in the presence of an armchair boundary. In the chiral Heisenberg transition, the spin rotation symmetry is also preserved in the presence of armchair boundaries. The fact that the symmetry remains intact ensures the vanishing of the Feynman diagram in Fig. 2. To illustrate, consider a Yukawa coupling of the form: $\psi^\dagger \Gamma \psi$, which transforms under a symmetry transformation S as $S^\dagger \Gamma S = -\Gamma$. This transformation property implies $\text{Tr}[\Gamma G] = 0$ because $\text{Tr}[\Gamma G] = \text{Tr}[\Gamma S G S^\dagger] = -\text{Tr}[\Gamma G]$. Here, we use the fact that the Green's function $G \sim \langle \psi \psi^\dagger \rangle$ [46] is invariant under the symmetry transformation S . Notably, previous studies of the GNY model [34, 35] did not account for this symmetry, leading to different results originated from the Feynman diagram in Fig. 2 (d).

The Kekulé VBS transition provides a counter example, because the presence of armchair boundaries explicitly breaks the translation symmetry under consideration. Consequently, the diagram in Fig. 2 (d) does not vanish. Moreover, the loss of translation symmetry introduces a linear coupling to the VBS order parameter at the boundary. This suggests that the Kekulé VBS transition in the presence of an armchair boundary belongs to the normal boundary condition of the chiral XY universality class. On the contrary, the $U(1)$ symmetry at the transition to a pair-density wave (PDW) superconducting state remains intact [47]. We leave the investigation of the PDW transition with possible boundary supersymmetric conformal field theory for an upcoming work.

Concluding remarks.— To conclude, we have investigated the boundary criticality of the GNY model in the context of condensed matter physics through explicit model calculations and RG analysis. Our RG analysis primarily focuses on the ordinary and special transitions. An important direction for future work is extending the RG calculations to the extraordinary transition [48–51], where the bare fermion Green's function must incorporate a finite mass term induced by the scalar field in the chiral Ising transition. For the chiral Heisenberg transition, it would be particularly interesting to explore the possibility of an extraordinary-log transition [52–57] in the presence of Dirac fermions. The GNY universality class has been studied in various experimental settings [14, 58–60]. In particular, the boundary exponent for fermions can be probed using scanning tunneling microscopy at the system's edge. Finally, it would be interesting to use determinant quantum Monte Carlo to simulate the lattice model (1) to explore boundary criticality, as it is free of the sign problem [61]. We leave this simulation to the future work.

Acknowledgements: We would like to thank Yang Ge for helpful discussions. The numerical mean-field calculation was performed using high-performance computational resources provided by the Louisiana Optical Network Infrastructure. This work is supported by a start-up fund (H. J. and S.-K. J.) and a COR Research Fellowship (S.-K. J.) at Tulane University.

* sjian@tulane.edu

- [1] N. Andrei, A. Bissi, M. Buican, J. Cardy, P. Dorey, N. Drukker, J. Erdmenger, D. Friedan, D. Fursaev, A. Konechny, C. Kristiansen, I. Makabe, Y. Nakayama, A. O'Bannon, R. Parini, B. Robinson, S. Ryu, C. Schmidt-Colinet, V. Schomerus, C. Schweigert, and G. Watts, *Boundary and defect cft: Open problems and applications* (2018), [arXiv:1810.05697 \[hep-th\]](https://arxiv.org/abs/1810.05697).
- [2] H. Diehl and S. Dietrich, Field-theoretical approach to static critical phenomena in semi-infinite systems, *Zeitschrift für Physik B Condensed Matter* **42**, 65 (1981).
- [3] H. Diehl and S. Dietrich, Multicritical behaviour at surfaces, *Zeitschrift für Physik B Condensed Matter* **50**, 117 (1983).
- [4] C. Domb and J. L. Lebowitz, eds., *PHASE TRANSITIONS AND CRITICAL PHENOMENA. VOL. 10* (1986).
- [5] H. W. Diehl, The Theory of boundary critical phenomena, *Int. J. Mod. Phys. B* **11**, 3503 (1997), [arXiv:cond-mat/9610143](https://arxiv.org/abs/cond-mat/9610143).
- [6] J. Cardy, *Scaling and renormalization in statistical physics*, Vol. 5 (Cambridge university press, 1996).
- [7] P. Liendo, L. Rastelli, and B. C. van Rees, The Bootstrap Program for Boundary CFT_d, *JHEP* **07**, 113, [arXiv:1210.4258 \[hep-th\]](https://arxiv.org/abs/1210.4258).
- [8] S. Giombi and H. Khanchandani, CFT in AdS and boundary RG flows, *JHEP* **11**, 118, [arXiv:2007.04955 \[hep-th\]](https://arxiv.org/abs/2007.04955).
- [9] J. Kondo, Resistance minimum in dilute magnetic alloys, *Progress of Theoretical Physics* **32**, 37 (1964), <https://academic.oup.com/ptp/article-pdf/32/1/37/5193092/32-1-37.pdf>.
- [10] I. Affleck and A. W. Ludwig, The kondo effect, conformal field theory and fusion rules, *Nuclear Physics B* **352**, 849 (1991).
- [11] J. M. Maldacena, The Large N limit of superconformal field theories and supergravity, *Adv. Theor. Math. Phys.* **2**, 231 (1998), [arXiv:hep-th/9711200](https://arxiv.org/abs/hep-th/9711200).
- [12] E. Witten, Anti-de Sitter space and holography, *Adv. Theor. Math. Phys.* **2**, 253 (1998), [arXiv:hep-th/9802150](https://arxiv.org/abs/hep-th/9802150).
- [13] S. S. Gubser, I. R. Klebanov, and A. M. Polyakov, Gauge theory correlators from noncritical string theory, *Phys. Lett. B* **428**, 105 (1998), [arXiv:hep-th/9802109](https://arxiv.org/abs/hep-th/9802109).
- [14] A. H. Castro Neto, F. Guinea, N. M. R. Peres, K. S. Novoselov, and A. K. Geim, The electronic properties of graphene, *Rev. Mod. Phys.* **81**, 109 (2009).
- [15] M. Z. Hasan and C. L. Kane, Colloquium: Topological insulators, *Rev. Mod. Phys.* **82**, 3045 (2010).
- [16] X.-L. Qi and S.-C. Zhang, Topological insulators and superconductors, *Rev. Mod. Phys.* **83**, 1057 (2011).
- [17] N. P. Armitage, E. J. Mele, and A. Vishwanath, Weyl and dirac semimetals in three-dimensional solids, *Rev. Mod. Phys.* **90**, 015001 (2018).
- [18] B. Q. Lv, T. Qian, and H. Ding, Experimental perspective on three-dimensional topological semimetals, *Rev. Mod. Phys.* **93**, 025002 (2021).
- [19] B. Rosenstein, H.-L. Yu, and A. Kovner, Critical exponents of new universality classes, *Phys. Lett. B* **314**, 381 (1993).
- [20] I. F. Herbut, Wilson-fisher fixed points in the presence of dirac fermions, *Modern Physics Letters B* **38**, 2430006 (2024), <https://doi.org/10.1142/S0217984924300060>.
- [21] D. J. Gross and A. Neveu, Dynamical symmetry breaking in asymptotically free field theories, *Phys. Rev. D* **10**, 3235 (1974).
- [22] J. Zinn-Justin, Four fermion interaction near four-dimensions, *Nucl. Phys. B* **367**, 105 (1991).
- [23] M. Moshe and J. Zinn-Justin, Quantum field theory in the large N limit: A Review, *Phys. Rept.* **385**, 69 (2003), [arXiv:hep-th/9707023](https://arxiv.org/abs/hep-th/9707023).

- th/0306133.
- [24] I. F. Herbut, V. Juričić, and O. Vafek, Relativistic mott criticality in graphene, *Phys. Rev. B* **80**, 075432 (2009).
 - [25] D. M. McAvity and H. Osborn, Energy momentum tensor in conformal field theories near a boundary, *Nucl. Phys. B* **406**, 655 (1993), [arXiv:hep-th/9302068](#).
 - [26] D. Carmi, L. Di Pietro, and S. Komatsu, A Study of Quantum Field Theories in AdS at Finite Coupling, *JHEP* **01**, 200, [arXiv:1810.04185 \[hep-th\]](#).
 - [27] C. P. Herzog and K.-W. Huang, Boundary Conformal Field Theory and a Boundary Central Charge, *JHEP* **10**, 189, [arXiv:1707.06224 \[hep-th\]](#).
 - [28] C. P. Herzog, K.-W. Huang, I. Shamir, and J. Virrueta, Superconformal Models for Graphene and Boundary Central Charges, *JHEP* **09**, 161, [arXiv:1807.01700 \[hep-th\]](#).
 - [29] V. Schaub, Spinors in (Anti-)de Sitter Space, *JHEP* **09**, 142, [arXiv:2302.08535 \[hep-th\]](#).
 - [30] J. Barrat, Line defect correlators in fermionic cft, in *Line Defects in Conformal Field Theory: From Weak to Strong Coupling* (Springer, 2025) pp. 157–191.
 - [31] A. Kakkar and S. Sarkar, Phases of theories with fermions in AdS, *JHEP* **06**, 009, [arXiv:2303.02711 \[hep-th\]](#).
 - [32] E. Brillaux, A. A. Fedorenko, and I. A. Gruzberg, Surface quantum critical phenomena in disordered Dirac semimetals, *Phys. Rev. B* **109**, 174204 (2024), [arXiv:2312.10790 \[cond-mat.dis-nn\]](#).
 - [33] X. Shen, Z. Wu, and S.-K. Jian, New boundary criticality in topological phases, [arXiv preprint arXiv:2407.15916 \(2024\)](#).
 - [34] S. Giombi, E. Helfenberger, and H. Khanchandani, Fermions in AdS and Gross-Neveu BCFT, *JHEP* **07**, 018, [arXiv:2110.04268 \[hep-th\]](#).
 - [35] C. P. Herzog and V. Schaub, Fermions in boundary conformal field theory: crossing symmetry and E-expansion, *JHEP* **02**, 129, [arXiv:2209.05511 \[hep-th\]](#).
 - [36] Note that the boundary condition of Dirac fermions has been extensively discussed in condensed matter physics [40, 62–64].
 - [37] Z.-X. Li, Y.-F. Jiang, and H. Yao, Fermion-sign-free Majorana-quantum-Monte-Carlo studies of quantum critical phenomena of Dirac fermions in two dimensions, *New J. Phys.* **17**, 085003 (2015), [arXiv:1411.7383 \[cond-mat.str-el\]](#).
 - [38] We set the velocity to be one due to the emergent Lorentz symmetry. The presence of the boundary will not affect the bulk renormalization.
 - [39] Our convention of the gamma matrices is different from e.g. Ref. [65], but the results do not depend on the convention of gamma matrices.
 - [40] L. Brey and H. A. Fertig, Electronic states of graphene nanoribbons studied with the dirac equation, *Phys. Rev. B* **73**, 235411 (2006).
 - [41] Notice that this is a tree-level analysis [2–4].
 - [42] S. Sorella, Y. Otsuka, and S. Yunoki, Absence of a spin liquid phase in the hubbard model on the honeycomb lattice, *Scientific reports* **2**, 992 (2012).
 - [43] F. F. Assaad and I. F. Herbut, Pinning the order: The nature of quantum criticality in the hubbard model on honeycomb lattice, *Phys. Rev. X* **3**, 031010 (2013).
 - [44] More precisely, the gamma matrices take the form $\gamma^\mu \otimes 1$ and the spin matrices are $1 \otimes s^i$.
 - [45] Z.-X. Li, Y.-F. Jiang, S.-K. Jian, and H. Yao, Fermion-induced quantum critical points, *Nature communications* **8**, 314 (2017).
 - [46] This should be distinguished from the propagator in (5), which is presented in a relativistic form $G \sim \langle \psi \bar{\psi} \rangle$. However, the discussion does not rely on the specific representation.
 - [47] S.-K. Jian, Y.-F. Jiang, and H. Yao, Emergent spacetime supersymmetry in 3d weyl semimetals and 2d dirac semimetals, *Phys. Rev. Lett.* **114**, 237001 (2015).
 - [48] A. J. Bray and M. A. Moore, Critical behaviour of semi-infinite systems, *J. Phys. A* **10**, 1927 (1977).
 - [49] H. W. Diehl and M. Smock, Critical behavior at supercritical surface enhancement: Temperature singularity of surface magnetization and order-parameter profile to one-loop order, *Phys. Rev. B* **47**, 5841 (1993).
 - [50] T. W. Burkhardt and H. W. Diehl, Ordinary, extraordinary, and normal surface transitions: Extraordinary-normal equivalence and simple explanation of $|T - T_c|^{2-\alpha}$ singularities, *Phys. Rev. B* **50**, 3894 (1994).
 - [51] X. Sun and S.-K. Jian, Boundary operator expansion and extraordinary phase transition in the tricritical o(n) model, [arXiv preprint arXiv:2501.06287 \(2025\)](#).
 - [52] M. A. Metlitski, Boundary criticality of the O(N) model in d = 3 critically revisited, *SciPost Phys.* **12**, 131 (2022), [arXiv:2009.05119 \[cond-mat.str-el\]](#).
 - [53] F. Parisen Toldin, Boundary critical behavior of the three-dimensional heisenberg universality class, *Phys. Rev. Lett.* **126**, 135701 (2021).
 - [54] M. Hu, Y. Deng, and J.-P. Lv, Extraordinary-log surface phase transition in the three-dimensional xy model, *Phys. Rev. Lett.* **127**, 120603 (2021).
 - [55] J. Padayasi, A. Krishnan, M. A. Metlitski, I. A. Gruzberg, and M. Meineri, The extraordinary boundary transition in the 3d O(N) model via conformal bootstrap, *SciPost Phys.* **12**, 190 (2022), [arXiv:2111.03071 \[cond-mat.stat-mech\]](#).
 - [56] X. Zou, S. Liu, and W. Guo, Surface critical properties of the three-dimensional clock model, *Phys. Rev. B* **106**, 064420 (2022).
 - [57] G. Cuomo and S. Zhang, Spontaneous symmetry breaking on surface defects, *JHEP* **03**, 022, [arXiv:2306.00085 \[hep-th\]](#).
 - [58] K. K. Gomes, W. Mar, W.-H. Ko, F. Guinea, and H. C. Manoharan, Designer Dirac fermions and topological phases in molecular graphene, *Nature* **483**, 306 (2012).
 - [59] C. Gutiérrez, C.-J. Kim, L. Brown, T. Schiros, D. Nordlund, E. B. Lochocki, K. M. Shen, J. Park, and A. N. Pasupathy, Imaging chiral symmetry breaking from kekulé bond order in graphene, *Nature Physics* **12**, 950 (2016).
 - [60] C. Bao, H. Zhang, T. Zhang, X. Wu, L. Luo, S. Zhou, Q. Li, Y. Hou, W. Yao, L. Liu, P. Yu, J. Li, W. Duan, H. Yao, Y. Wang, and S. Zhou, Experimental evidence of chiral symmetry breaking in kekulé-ordered graphene, *Phys. Rev. Lett.* **126**, 206804 (2021).
 - [61] Z.-X. Li, Y.-F. Jiang, and H. Yao, Solving the fermion sign problem in quantum monte carlo simulations by majorana representation, *Phys. Rev. B* **91**, 241117 (2015).
 - [62] A. R. Akhmerov and C. W. J. Beenakker, Boundary conditions for dirac fermions on a terminated honeycomb lattice, *Phys. Rev. B* **77**, 085423 (2008).
 - [63] Z. Faraei, T. Farajollahpour, and S. A. Jafari, Green’s function of semi-infinite weyl semimetals, *Phys. Rev. B* **98**, 195402 (2018).
 - [64] O. Shtanko and L. Levitov, Robustness and universality of surface states in dirac materials, *Proceedings of the National Academy of Sciences* **115**, 5908 (2018), <https://www.pnas.org/doi/pdf/10.1073/pnas.1722663115>.
 - [65] N. Zerf, L. N. Mihaila, P. Marquard, I. F. Herbut, and M. M. Scherer, Four-loop critical exponents for the Gross-Neveu-Yukawa models, *Phys. Rev. D* **96**, 096010 (2017), [arXiv:1709.05057 \[hep-th\]](#).
 - [66] T. Nishioka, Y. Okuyama, and S. Shimamori, Method of images in defect conformal field theories, *Phys. Rev. D* **106**, L081701

(2022).

[67] I. M. Gelfand and G. E. Shilov, *Generalized Functions: Volume I, Properties and Operations* (Academic Press, New York,

1964).

[68] S.-K. Jian and H. Yao, Fermion-induced quantum critical points in two-dimensional dirac semimetals, *Phys. Rev. B* **96**, 195162 (2017).

SUPPLEMENTAL MATERIAL

I. MEAN FIELD THEORY OF THE HONEYCOMB tV MODEL

In this section, we detail the mean field theory calculation of the phase diagram reported in the main text. We consider the Hamiltonian (1) for spinless fermions on honeycomb lattice with armchair boundaries:

$$H = -t \sum_{\langle ij \rangle} (c_i^\dagger c_j + h.c.) + V_{\text{bulk}} \sum'_{\langle ij \rangle} \left(n_i - \frac{1}{2} \right) \left(n_j - \frac{1}{2} \right) + V_{\text{bdy}} \sum''_{\langle ij \rangle} \left(n_i - \frac{1}{2} \right) \left(n_j - \frac{1}{2} \right),$$

where V_{bulk} (V_{bdy}) represents the interaction strength on bulk (boundary) bonds, and $\langle ij \rangle$ denotes the bonds. To compute the phase diagram, we use the following ansatz for the mean-field Hamiltonian:

$$H_{\text{mf}} [\{\phi_{\text{bulk}}^i, \phi_{\text{bdy}}^j\}] = -t \sum_{\langle ij \rangle} (c_i^\dagger c_j + h.c.) + \sum'_i \phi_{\text{bulk}}^i (-1)^{s(i)} n_i + \sum''_i \phi_{\text{bdy}}^i (-1)^{s(i)} n_i, \quad (\text{S1})$$

Here, $s(i) = 0, 1$ at two sublattices, and the sum \sum'_i and \sum''_i extend over the sites on bulk and boundary, respectively. $\phi_{\text{bulk/bdy}}^i$ denotes a charge density wave (CDW) order ansatz. Due to the symmetry of the armchair lattice, the order will still respect the translation symmetry along the y axis while break the translation symmetry along the x axis. This is illustrated in Fig. S1, where the dashed box denotes a unit cell of the CDW order in a lattice with $L = 4$. Here L represents the length along the x direction.

The CDW order is determined by the optimization of the mean-field ground state energy, as detailed in the following. Since the ground state of the mean-field Hamiltonian (the mean-field ground state) is a Gaussian state, its energy can be obtained by calculating the correlation matrix, whose elements are defined as

$$\Gamma_{i,j} \equiv \langle c_i^\dagger c_j \rangle_{\text{mf}} \equiv \langle \Psi_{\text{mf}} | c_i^\dagger c_j | \Psi_{\text{mf}} \rangle, \quad \Psi_{\text{mf}} \text{ is the ground state of the mean-field Hamiltonian (S1)}. \quad (\text{S2})$$

We focus on the half-filling sector. In the diagonalized basis, the diagonal elements of the correlation matrix follow the Fermi-Dirac distribution and at zero temperature we have:

$$\Gamma^D = \begin{pmatrix} 0 & 0 & \cdots & 0 & 0 \\ 0 & 0 & \cdots & 0 & 0 \\ \vdots & \vdots & \ddots & 0 & 0 \\ 0 & 0 & \cdots & 1 & 0 \\ 0 & 0 & \cdots & 0 & 1 \end{pmatrix}, \quad (\text{S3})$$

where Γ^D is the correlation matrix in the diagonal basis. We have arranged the eigen-energy in descending order, which implies that the upper (lower) half of the diagonal element Γ^D is zero (one) in the half-filling sector. Denoting the unitary transformation that diagonalize the mean-field Hamiltonian as U (i.e., $Ud = c$, with c the normal basis and d the diagonalized basis), the element of correlation matrix is

$$\Gamma_{i,j} = \langle c_i^\dagger c_j \rangle_{\text{mf}} = \sum_{\alpha, \beta} \langle d_\alpha^\dagger U_{i\alpha}^* U_{j\beta} d_\beta \rangle_{\text{mf}} = \sum_{\alpha, \beta} U_{i\alpha}^* U_{j\beta} \langle d_\alpha^\dagger d_\beta \rangle_{\text{mf}} = (U^* \Gamma^D U^T)_{i,j}, \quad (\text{S4})$$

where in the last step, we used the fact that correlation matrix in the diagonalized basis only has diagonal components. With this, the mean-field ground state energy can be written as,

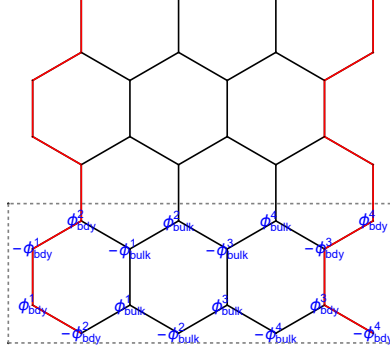
$$\begin{aligned} E [\{\phi_{\text{bulk}}^i, \phi_{\text{bdy}}^j\}] = \langle H \rangle_{\text{mf}} = & -t \sum_{\langle ij \rangle} (\Gamma_{i,j} + \Gamma_{j,i}) + V_{\text{bulk}} \sum'_{\langle ij \rangle} \left(\left(\Gamma_{i,i} - \frac{1}{2} \right) \left(\Gamma_{j,j} - \frac{1}{2} \right) - \Gamma_{i,j} \Gamma_{j,i} \right) \\ & + V_{\text{bdy}} \sum''_{\langle ij \rangle} \left(\left(\Gamma_{i,i} - \frac{1}{2} \right) \left(\Gamma_{j,j} - \frac{1}{2} \right) - \Gamma_{i,j} \Gamma_{j,i} \right), \end{aligned} \quad (\text{S5})$$

where correlation matrix $\Gamma_{j,i}$ is the function of $\phi_{\text{bulk/bdy}}^i$. We vary the CDW order to get the minimal of the mean-field ground state energy:

$$\left. \frac{\delta E [\{\phi_{\text{bulk}}^i, \phi_{\text{bdy}}^j\}]}{\delta \phi_{\text{bulk}}^i} \right|_{\phi_{\text{bulk/bdy}} = \phi_{\text{bulk/bdy}}^*} = \left. \frac{\delta E [\{\phi_{\text{bulk}}^i, \phi_{\text{bdy}}^j\}]}{\delta \phi_{\text{bdy}}^j} \right|_{\phi_{\text{bulk/bdy}} = \phi_{\text{bulk/bdy}}^*} = 0, \quad (\text{S6})$$

where $\{\phi_{\text{bulk}}^{i*}, \phi_{\text{bdy}}^{j*}\}$ denote the CDW order parameters corresponding to the minimal energy.

In our calculation, we focus on a lattice geometry with the length perpendicular to the armchair boundary is given by $L = 3\mathbb{Z} + 1$, so that the free fermion is gapless [40]. We used $L = 25, 37, 49$ and a similar number for the momentum points along y direction.



Supplementary Figure S1. Illustration of the unit cell in a honeycomb lattice with armchair boundaries, along with the corresponding order parameters. The interaction strength in black (red) bonds correspond to V_{bulk} (V_{edge}). The gray dashed line delineates a unit cell. ϕ denotes the CDW order parameter, where ϕ_{bdy} (ϕ_{bulk}) represents the order on the boundary (in the bulk). The lattice is periodic along the y axis, while the lattice length along the x axis is chosen to be $L = 4$ for an illustration. In the mean-field calculation, L ranges from 25 to 49.

II. DERIVATION OF THE BOUNDARY CONDITION AND PROPAGATORS

In this section, we derive the boundary condition for the Dirac fermion and the propagators.

A. Boundary condition

We give a brief derivation of the boundary condition for the Dirac fermion [40]. At the ordinary and the special transition, the order parameter remains zero. Hence, the bare propagator will be given by the free model. $H_0 = -t \sum_{\langle ij \rangle} (c_i^\dagger c_j + h.c.)$. It is well-known that the free tight binding model, describing fermions hopping on a honeycomb lattice, features two gapless points at K and K' , respectively [14]. To be concrete, we choose the unit cell vectors to be $a_1 = (1, 0)$ and $a_2 = (\frac{1}{2}, \frac{\sqrt{3}}{2})$, then consequently the two valleys are $K = \frac{4\pi}{3}(1, 0)$ and $K' = \frac{4\pi}{3}(-1, 0)$. Near these points, adopting $\mathbf{k} \cdot \mathbf{P}$ expansion, we arrive at a continuous model for the Dirac fermion, $\mathcal{H} = k_x \sigma^x \tau^z + k_y \sigma^y$ with the basis $\psi = (\psi_{A,K}, \psi_{B,K}, \psi_{A,K'}, \psi_{B,K'})^T$.

Let us consider an armchair boundary along y direction, as illustrated in Fig. S1. With the translation symmetry breaking in x direction, the eigenstate satisfies the Dirac equation,

$$(-i\partial_x \sigma^x \tau^z + k_y \sigma^y) \psi(x) = E \psi(x), \quad (\text{S7})$$

where E denotes the eigen-energy. This equation is supplemented with proper boundary conditions at the armchair boundary. The boundary condition requires the wave function amplitudes vanish at those sites (not shown) that would be connecting to the boundary (shown in the red color). We set the coordinates of these sites to be $x = 0$ for convenience, then we have $\Psi_\sigma(x=0) = 0$ for $\sigma = A, B$, where $\Psi_\sigma(x)$ can be expressed in terms of the Dirac fermion,

$$\Psi_\sigma(x) = \psi_{\sigma,K}(x) e^{iK \cdot x} + \psi_{\sigma,K'}(x) e^{iK' \cdot x}. \quad (\text{S8})$$

Therefore, in terms of the Dirac fermion, this boundary condition reads $\psi_{\sigma,K}(0) + \psi_{\sigma,K'}(0) = 0$, which can be expressed compactly in a matrix form,

$$\tau^x \psi(x) = -\psi(x). \quad (\text{S9})$$

The boundary condition mixes two valleys, because the fermion can scatter between valleys due to translation symmetry breaking at the boundary.

It will be convenient to work in a relativistic convention. To this end, we choose the following convention for the gamma matrix,

$$\gamma^0 = \tau^y \sigma^x, \gamma^1 = \tau^x, \gamma^2 = \tau^y \sigma^z, \gamma^3 = \tau^z, \gamma^5 = \tau^y \sigma^y. \quad (\text{S10})$$

The free Dirac Lagrangian becomes $\mathcal{L} = \bar{\psi} \partial_\mu \gamma^\mu \psi$, with $\bar{\psi} = \psi^\dagger \gamma^0$, and the boundary condition becomes $\gamma^1 \psi(0) = -\psi(0)$.

There is a more universal way to determine the boundary condition, without relying on the free model. Suppose the armchair boundary condition is given by a matrix M . This matrix should obey a few properties: 1) it anticommutes with the current in the x direction because the perpendicular current vanishes at the boundary, 2) it commutes with the current in the y direction, as the translation is preserved in the y direction, 3) it commutes with the mirror symmetry $y \rightarrow -y$ because the armchair boundary respects this mirror symmetry, 4) it further commutes with the particle-hole symmetry. Hence, we have

$$\{M, \tau^z \sigma^x\} = 0, \quad [M, \sigma^y] = 0, \quad [M, \sigma^x] = 0, \quad [M, \sigma^x K] = 0, \quad (\text{S11})$$

where K denotes complex conjugation. It is easy to check that the only matrix with these properties is $\gamma^1 = \tau^x$. One can show that this boundary condition actually respects conformal symmetry [32].

The above analysis gives the Dirichlet boundary condition for a semi-infinite geometry with an armchair boundary at $x = 0$. It is enough for our RG calculation. While, in our mean-field calculation, the ribbon geometry has another armchair boundary. More specifically, if the honeycomb lattice with finite length L in x direction, the boundary conditions require the Dirac field should satisfy

$$\psi_{\sigma,K}(0) + \psi_{\sigma,K'}(0) = 0, \quad (\text{S12})$$

$$\psi_{\sigma,K} \left(L + \frac{1}{2} \right) e^{i\frac{4\pi}{3}(L+\frac{1}{2})} + \psi_{\sigma,K'} \left(L + \frac{1}{2} \right) e^{-i\frac{4\pi}{3}(L+\frac{1}{2})} = 0, \quad (\text{S13})$$

for the Dirichlet condition at the two armchair boundaries. It has been shown that with this boundary condition, the eigen-energy is [40]

$$E_n = \pm \sqrt{k_n^2 + k_y^2}, \quad k_n = 2\pi \left(\frac{1}{3} - \frac{n}{2L+1} \right), \quad n = 0, \dots, L-1. \quad (\text{S14})$$

For $L = 3\mathbb{Z} + 1$, the spectrum is gapless at $k_n = (2L+1)/3$. Our mean-field calculation has focused on these special lengths to better characterize the gapless states in the thermodynamic limit.

B. Propagator of Dirac fermion

With the Lagrangian and the boundary condition derived from the previous subsection, we calculate the bare propagator in this subsection. For generality, we consider a 3+1-dimensional Dirac fermion by including the k_z direction. The propagator satisfies the following different equation,

$$(i\omega\gamma^0 + \gamma^x \partial_x + ik_y \gamma^2 + ik_z \gamma^3)G(k, x, x') = \delta(x - x'), \quad (\text{S15})$$

where k denotes the momentum along the directions with translational symmetry. Expanding the matrix multiplication, one can show that (S15) can be written as

$$i\tau k_z G_{\tau\tau}^{\sigma\sigma} + (\partial_x + \tau\sigma k_y)G_{\tau\tau}^{\sigma\sigma} + \tau\omega G_{\tau\tau}^{\bar{\sigma}\sigma} = \delta(x - x'), \quad (\text{S16})$$

$$i\tau k_z G_{\tau\tau}^{\bar{\sigma}\sigma} + (\partial_x - \tau\sigma k_y)G_{\tau\tau}^{\bar{\sigma}\sigma} + \tau\omega G_{\tau\tau}^{\sigma\sigma} = 0, \quad (\text{S17})$$

$$-i\tau k_z G_{\tau\tau}^{\sigma\sigma} + (\partial_x - \tau\sigma k_y)G_{\tau\tau}^{\sigma\sigma} - \tau\omega G_{\tau\tau}^{\bar{\sigma}\sigma} = 0, \quad (\text{S18})$$

$$-i\tau k_z G_{\tau\tau}^{\bar{\sigma}\sigma} + (\partial_x + \tau\sigma k_y)G_{\tau\tau}^{\bar{\sigma}\sigma} - \tau\omega G_{\tau\tau}^{\sigma\sigma} = 0, \quad (\text{S19})$$

where $\sigma = \pm$, $\bar{\sigma} = -\sigma$, $\tau = \pm$, $\bar{\tau} = -\tau$ denote the sublattice and valley space, respectively. From (S18) and (S19), we obtain

$$G_{\tau\tau}^{\sigma\sigma} = \frac{(\partial_x - \tau\sigma k_y)G_{\tau\tau}^{\sigma\sigma} - \tau\omega G_{\tau\tau}^{\bar{\sigma}\sigma}}{i\tau k_z}, \quad G_{\tau\tau}^{\bar{\sigma}\sigma} = \frac{(\partial_x + \tau\sigma k_y)G_{\tau\tau}^{\bar{\sigma}\sigma} - \tau\omega G_{\tau\tau}^{\sigma\sigma}}{i\tau k_z}. \quad (\text{S20})$$

Plugging them back into (S16) and (S17), we arrive at

$$(\partial_x^2 - q^2)G_{\tau\tau}^{\sigma\sigma} = i\tau k_z \delta(x - x'), \quad (\text{S21})$$

$$(\partial_x^2 - q^2)G_{\tau\tau}^{\bar{\sigma}\sigma} = 0, \quad (\text{S22})$$

where we defined $q^2 = \omega^2 + k_y^2 + k_z^2$. The solutions to these equations are then given by:

$$G_{\tau\tau}^{\sigma\sigma}(k, x, x') = C_{\tau\tau}^{\sigma\sigma}(k, x')e^{-qx} + \frac{i\tau k_z}{2q}e^{-q|x-x'|}, \quad (\text{S23})$$

$$G_{\tau\tau}^{\bar{\sigma}\sigma}(k, x, x') = D_{\tau\tau}^{\bar{\sigma}\sigma}(k, x')e^{-qx}, \quad (\text{S24})$$

where $C_{\tau\tau}^{\sigma\sigma}(k, x')$ and $D_{\tau\tau}^{\bar{\sigma}\sigma}(k, x')$ are functions of x' to be determined. The boundary condition leads to $-\gamma^1 G(k, 0, x) = G(k, 0, x)$. Explicitly, this yield

$$-G_{\tau\tau}^{\sigma\sigma}(k, 0, x) = G_{\tau\tau}^{\sigma\sigma}(k, 0, x), \quad -G_{\tau\tau}^{\bar{\sigma}\sigma}(k, 0, x) = G_{\tau\tau}^{\bar{\sigma}\sigma}(k, 0, x). \quad (\text{S25})$$

Hence, solving simultaneously the equations (S16)–(S19) and (S23)–(S25), we obtain the solutions

$$G_{\tau\tau}^{\sigma\sigma}(k, x, x') = \frac{i\tau k_z}{2q}e^{-q|x-x'|} + \left(-\frac{1}{2} + \frac{\sigma\tau k_y}{2q}\right)e^{-q(x+x')}, \quad (\text{S26})$$

$$G_{\tau\tau}^{\bar{\sigma}\sigma}(k, x, x') = \frac{\omega\tau}{2q}e^{-q(x+x')}, \quad (\text{S27})$$

$$G_{\tau\tau}^{\sigma\sigma}(k, x, x') = \left[-\frac{\tau\sigma k_y}{2q} - \frac{1}{2}\text{sgn}(x - x')\right]e^{-q|x-x'|} - \frac{i\tau k_z}{2q}e^{-q(x+x')}, \quad (\text{S28})$$

$$G_{\tau\tau}^{\bar{\sigma}\sigma}(k, x, x') = -\frac{\tau\omega}{2q}e^{-q|x-x'|}. \quad (\text{S29})$$

In matrix form, the propagator can be compactly expressed as

$$G(k, x, x') = G_b(k, x, x') + G_s(k, x, x'), \quad (\text{S30})$$

$$G_b(k, x, x') = \left[\frac{i\cancel{k}}{2q} - \frac{\gamma^1}{2}\text{sgn}(x - x')\right]e^{-q|x-x'|}, \quad (\text{S31})$$

$$G_s(k, x, x') = -\gamma^1 \left(\frac{i\cancel{k}}{2q} + \frac{\gamma^1}{2}\right)e^{-q(x+x')}, \quad (\text{S32})$$

where $\cancel{k} = k_\mu \gamma^\mu$ for $\mu \neq 1$. G_b and G_s correspond to contributions with and without translational symmetry, respectively.

To simplify the calculation of the fermion loop, we also transform the propagator to the real space via Fourier transformation. The Fourier transformation in $d - 1$ flat space read

$$\int d^{d-1}y \frac{e^{iq \cdot y}}{(y^2 + x^2)^\Delta} = \frac{2^{\frac{d+1}{2}-\Delta} \pi^{\frac{d-1}{2}}}{\Gamma(\Delta)} \left(\frac{q}{|x|}\right)^{\Delta-\frac{d-1}{2}} K_{\Delta-\frac{d-1}{2}}(q|x|). \quad (\text{S33})$$

where K is the modified Bessel function. This transformation yields

$$G_b(y, x, x') = \frac{\Gamma(\frac{d}{2})}{2\pi^{d/2}} \frac{-\not{y} - (x - x')\gamma^1}{(y^2 + (x - x')^2)^{d/2}}, \quad (\text{S34})$$

$$G_s(y, x, x') = \frac{\Gamma(\frac{d}{2})}{2\pi^{d/2}} \gamma^1 \frac{-\not{y} + (x + x')\gamma^1}{(y^2 + (x + x')^2)^{d/2}}, \quad (\text{S35})$$

where y denotes the coordinates in the direction with translation symmetry.

For completeness, we also present the boson propagator in the real space,

$$D_b(y, x, x') = \frac{\Gamma(\frac{d-2}{2})}{4\pi^{d/2}} \frac{1}{(y^2 + (x - x')^2)^{\frac{d-2}{2}}}, \quad (\text{S36})$$

$$D_s(y, x, x') = \frac{\Gamma(\frac{d-2}{2})}{4\pi^{d/2}} \frac{1}{(y^2 + (x + x')^2)^{\frac{d-2}{2}}}. \quad (\text{S37})$$

C. Method of image

In addition to the detailed derivation of the propagator, one can use the method of image [66] to obtain the propagator in the Dirichlet and Neumann boundary conditions. According to the method of image, the propagator of a scalar in a semi-infinite space \mathcal{M} is

$$\langle \phi(x_1^\mu) \phi(x_2^\mu) \rangle_{\mathcal{M}} = \langle \phi(x_1^\mu) \phi(x_2^\mu) \rangle_{\mathcal{M}'} + w \langle \phi(\bar{x}_1^\mu) \phi(x_2^\mu) \rangle_{\mathcal{M}'}, \quad (\text{S38})$$

where \bar{x}^μ is the image of x^μ by a reflection across the boundary plane $\partial\mathcal{M}$, and $w = 1$ ($w = -1$) when ϕ satisfied Neumann (Dirichlet) boundary condition respectively. $\langle \cdot \rangle_{\mathcal{M}}$ ($\langle \cdot \rangle_{\mathcal{M}'}$) denotes the propagator in the semi-infinite (infinite) space. Hence, the propagator of the boson is

$$D(k, x, x') = D_b(k, x, x') + w D_b(k, \bar{x}, x'), \quad D_b(k, x, x') = \frac{e^{-q|x-x'|}}{2q}, \quad (\text{S39})$$

where $q^2 = \sum_{\mu \neq 1} k_\mu^2$ and D_b is the propagator in the infinite space. $\bar{x} = -x$ is the image point with respect to the boundary, and k denotes the momentum in the space parallel to the boundary. For spinor field, we can generalize the method of image

$$\langle \psi(x_1^\mu) \bar{\psi}(x_2^\mu) \rangle_{\mathcal{M}} = \langle \psi(x_1^\mu) \bar{\psi}(x_2^\mu) \rangle_{\mathcal{M}'} + w \gamma^1 \langle \psi(\bar{x}_1^\mu) \bar{\psi}(x_2^\mu) \rangle_{\mathcal{M}'} \quad (\text{S40})$$

where γ^1 is the reflection matrix across the x direction. Hence, the propagator of the Dirac fermion in the semi-infinite space is

$$G(k, x, x') = G_b(k, x, x') + w \gamma^1 G_b(k, \bar{x}, x'), \quad G_b(k, x, x') = \left(\frac{i\mathbf{k}}{2q} - \frac{\gamma^1}{2} \text{sgn}(x - x') \right) e^{-q|x-x'|}. \quad (\text{S41})$$

For the Dirichlet boundary condition $w = -1$, it is consistent with the result from the last subsection (S30).

III. RENORMALIZATION GROUP CALCULATION OF CHIRAL ISING UNIVERSALITY CLASS

In this section, we detail the RG calculation for the chiral Ising universality class. The action for the chiral Ising universality class reads,

$$S = \int_{\mathcal{M}} d^d x \left(\sum_j \bar{\psi}_j \gamma^\mu \partial_\mu \psi_j + \frac{1}{2} (\partial_\mu \phi)^2 + \frac{\lambda}{4!} \phi^4 - ig \sum_j \phi \bar{\psi}_j \gamma^5 \psi_j \right), \quad (\text{S42})$$

where ψ_j represents the Dirac fermion fields and ϕ is the order parameter field. ∂_μ denotes derivatives regarding (imaginary) time $x_0 \equiv \tau$ and space $x_i, i = 1, \dots, d-1$. γ_μ are gamma matrices: $\gamma^0 = \tau^y \sigma^x$, $\gamma^1 = \tau^x$, $\gamma^2 = \tau^y \sigma^z$, $\gamma^3 = \tau^z$, and $\gamma^5 = \tau^y \sigma^y$, and $\bar{\psi} = \psi^\dagger \gamma^0$. Note that, to make our theory more general, we extend the fermion sector to include N flavors, denoted as ψ_j for $j = 1, \dots, N$. The parameters λ and g represent the quartic boson self-interaction and the fermion-boson Yukawa coupling, respectively. The field theory is located in a d -dimensional semi-infinite spacetime, $\mathcal{M} = \{x_\mu | x_1 > 0\}$ where the boundary is $\partial\mathcal{M} = \{x_\mu | x_1 = 0\}$. We denote the hyperspace parallel to the boundary as y and the coordinate perpendicular to the boundary as x . The boundary condition for the Dirac fermion arises from the vanishing of the lattice fermion outside the lattice sites, enforcing a Dirichlet boundary condition. The boundary condition for the Dirac fermion field is $-\gamma^1 \psi|_{x=0} = \psi|_{x=0}$. The bulk $4 - \epsilon$ RG analysis for the chiral Ising universality is well-known [65], here we present the RG factors in the one-loop order,

$$Z_\phi = 1 - \frac{Ng^2}{4\pi^2\epsilon}, \quad Z_\psi = 1 - \frac{g^2}{16\pi^2\epsilon}, \quad (\text{S43})$$

$$Z_g = 1 + \frac{(3+2N)g^2}{16\pi^2\epsilon}, \quad Z_\lambda = 1 + \frac{Ng^2}{2\pi^2\epsilon} + \frac{3\lambda}{16\pi^2\epsilon} - \frac{N3g^4}{\lambda\pi^2\epsilon}, \quad (\text{S44})$$

which are defined as

$$\phi = \sqrt{Z_\phi} \phi_R, \quad \psi = \sqrt{Z_\psi} \psi_R, \quad g = \mu^{\epsilon/2} Z_g g_R, \quad \lambda = \mu^\epsilon Z_\lambda \lambda_R \quad (\text{S45})$$

where $\hat{\phi}_R, \hat{\psi}_R, g_R$ and λ_R denote the renormalized quantities. Consequently, the RG equation at the one-loop order reads,

$$\frac{d\lambda}{d \log \mu} = -\epsilon \lambda + \frac{N\lambda g^2}{2\pi^2} + \frac{3\lambda^2}{16\pi^2} - \frac{3Ng^4}{\pi^2}, \quad (\text{S46})$$

$$\frac{dg}{d \log \mu} = -\frac{\epsilon}{2} g + \frac{(3+2N)g^3}{16\pi^2}. \quad (\text{S47})$$

This leads to the chiral Ising fixed point at

$$\lambda^* = \frac{8\pi^2 [(3 - 2N) + \sqrt{4N^2 + 132N + 9}]}{3(2N + 3)}\epsilon, \quad g^* = \frac{2\pi\sqrt{\epsilon}}{\sqrt{3/2 + N}}. \quad (\text{S48})$$

Furthermore, the scaling dimensions for the boson and fermion are, respectively, given by

$$\Delta_\phi = 1 - \frac{3}{6 + 4N}\epsilon, \quad \Delta_\psi = \frac{3}{2} - \frac{5 + 4N}{12 + 8N}\epsilon. \quad (\text{S49})$$

where N is the flavor of the four-component Dirac fermion. In the following, we will calculate the boundary critical exponents at the ordinary and special transition. The fermion satisfies the Dirichlet boundary condition at both transitions, so the bare fermion propagator is (S41) with $w = -1$.

A. Ordinary transition

At the ordinary transition, the boson field obeys the Dirichlet boundary conditions. Hence, the boson propagator is (S39) with $w = -1$. The RG factors for the boundary fields are defined by [3],

$$\hat{\phi} = \sqrt{Z_\phi Z_{\partial\hat{\phi}}}\partial\hat{\phi}_R, \quad \hat{\psi} = \sqrt{Z_\psi Z_{\hat{\psi}}}\hat{\psi}_R, \quad (\text{S50})$$

where $\hat{\phi}_R$ and $\partial\hat{\phi}_R$ denote the renormalized fields.

As stated in the main text, to get the scaling dimension for $\partial\hat{\phi}$, we consider the correction to the correlation function $\langle\phi\partial\hat{\phi}\rangle$. At the tree-level, the correlation is given by

$$\langle\phi(p, x)\partial_x\hat{\phi}(p', 0)\rangle = (2\pi)^{d-1}\delta(p + p')e^{px}. \quad (\text{S51})$$

At the one-loop level, the correction from the fermions, illustrated in the Feynman diagram Fig. 2 (a), is

$$\int dx_1 dx_2 D(p, x, x_1) G_2(p, x_1, x_2) [\partial_x D(p, x_2, x)]_{x=0}. \quad (\text{S52})$$

where G_2 denotes the fermion loop,

$$\begin{aligned} G_2(p, x_1, x_2) &= - \int d^{d-1}y e^{-ip \cdot y} \text{Tr} [(-i\gamma^5)G(y, x_1, x_2)(-i\gamma^5)G(-y, x_2, x_1)] \\ &= \frac{\Gamma(\frac{d}{2})^2}{\pi^d} \int d^{d-1}y e^{-ip \cdot y} \left[\frac{1}{(y^2 + (x_1 - x_2)^2)^{d-1}} + \frac{1}{(y^2 + (x_1 + x_2)^2)^{d-1}} \right] \end{aligned} \quad (\text{S53})$$

$$\rightarrow \frac{1}{8\pi^2} (2|x_1 - x_2|^{-3+\epsilon} - q^2|x_1 - x_2|^{-1+\epsilon}) + \frac{1}{8\pi^2} (2(x_1 + x_2)^{-3+\epsilon} - q^2(x_1 + x_2)^{-1+\epsilon}), \quad (\text{S54})$$

where in the last line, we perform the Fourier transformation using (S33), and then isolate the pole. To evaluate the divergences, we use the properties of the generalized function [3, 67]. For any function φ , a generalized function x^λ with $\text{Re}\lambda > -n - 1$ has the poles at $\lambda = -1, -2, \dots$ given by [67]

$$\int_0^\infty dx x^\lambda \varphi(x) = \sum_{k=1}^n \frac{\varphi^{(k-1)}(0)}{(k-1)!(\lambda + k)}. \quad (\text{S55})$$

In particular, the residue is $\varphi^{(k-1)}(0)/(k-1)!$ at $\lambda = -k$. Generalizing this result, we have

$$\int dx_1 dx_2 (x_1 + x_2)^{-3+\epsilon} \varphi(x_1, x_2) = \frac{1}{2\epsilon} [\varphi^{(1,0)}(0, 0) + \varphi^{(0,1)}(0, 0)], \quad (\text{S56})$$

$$\int dx_1 dx_2 |x_1 - x_2|^{-3+\epsilon} \varphi(x_1, x_2) = \frac{1}{\epsilon} \int_0^\infty dx [\varphi^{(2,0)}(x, x) + \varphi^{(0,2)}(x, x)], \quad (\text{S57})$$

$$\int dx_1 dx_2 |x_1 - x_2|^{-1+\epsilon} \varphi(x_1, x_2) = \frac{2}{\epsilon} \int_0^\infty dx \varphi(x, x), \quad (\text{S58})$$

where we used the shorthand notation

$$\varphi^{(n,m)}(x_1, x_2) = \frac{\partial^n}{\partial x_1^n} \frac{\partial^m}{\partial x_2^m} \varphi(x_1, x_2). \quad (\text{S59})$$

And there is not a pole in ϵ at $m = 1$ for $(x_1 + x_2)^{-1+\epsilon}$.

Using these result, we can evaluate the integration in (S52) and obtain the divergence

$$\int dx_1 dx_2 D(p, x, x_1) G_2(p, x_1, x_2) [\partial_x D(p, x_2, x)]_{x=0} = -\frac{e^{-px}}{8\pi^2\epsilon}. \quad (\text{S60})$$

Combining the result from the pure boson contribution [3], we arrive at the correction to the boson correlation function,

$$\langle \phi(p, x) \partial_x \phi(p', 0) \rangle = (2\pi)^{d-1} \delta(p + p') e^{-px} \left(1 + \frac{\lambda}{32\pi^2\epsilon} - \frac{Ng^2}{8\pi^2\epsilon} \right). \quad (\text{S61})$$

Next, to obtain the scaling dimension of the boundary fermion $\hat{\psi}$, let's consider the correction to the correlation function $\langle \psi \hat{\psi} \rangle$. The one-loop correction from the Feynman diagram Fig. 2 (b) leads to

$$\int dx_1 dx_2 G(k, x, x_1) \tilde{G}_2(k, x_1, x) G(k, x_2, 0), \quad (\text{S62})$$

where $\tilde{G}_2(k, x_1, x_2)$ is given by Fourier transformation

$$\tilde{G}_2(k, x_1, x_2) = \int d^{d-1}y e^{-ik \cdot y} (-i\gamma^5) G(y, x_1, x_2) (-i\gamma^5) D(y, x_1, x_2). \quad (\text{S63})$$

For computational convenience, we divide \tilde{G}_2 into the following four terms,

$$G_b D_b = \frac{\Gamma(\frac{d}{2})\Gamma(\frac{d-2}{2})}{8\pi^d} \frac{-\not{y} - (x_1 - x_2)\gamma^1}{(y^2 + (x_1 - x_2)^2)^{d-1}}, \quad (\text{S64})$$

$$G_s D_s = \frac{\Gamma(\frac{d}{2})\Gamma(\frac{d-2}{2})}{8\pi^d} \gamma^1 \frac{-\not{y} + (x_1 + x_2)\gamma^1}{(y^2 + (x_1 + x_2)^2)^{d-1}}, \quad (\text{S65})$$

$$\begin{aligned} G_b D_s &= \frac{\Gamma(\frac{d}{2})\Gamma(\frac{d-2}{2})}{8\pi^d} \frac{-\not{y} - (x_1 - x_2)\gamma^1}{(y^2 + (x_1 - x_2)^2)^{d/2} (y^2 + (x_1 + x_2)^2)^{d/2-1}}, \\ &= \frac{\Gamma(d-1)}{8\pi^d} \int_0^1 du u^{d/2-1} (1-u)^{d/2-2} \frac{-\not{y} - (x_1 - x_2)\gamma^1}{(y^2 + x_1^2 + x_2^2 + 2(1-2u)x_1x_2)^{d-1}}, \end{aligned} \quad (\text{S66})$$

$$\begin{aligned} G_s D_b &= \frac{\Gamma(\frac{d}{2})\Gamma(\frac{d-2}{2})}{8\pi^d} \gamma^1 \frac{-\not{y} + (x_1 + x_2)\gamma^1}{(y^2 + (x_1 + x_2)^2)^{d/2} (y^2 + (x_1 - x_2)^2)^{d/2-1}}, \\ &= \frac{\Gamma(d-1)}{8\pi^d} \int_0^1 du u^{d/2-1} (1-u)^{d/2-2} \gamma^1 \frac{-\not{y} + (x_1 + x_2)\gamma^1}{(y^2 + x_1^2 + x_2^2 - 2(1-2u)x_1x_2)^{d-1}}. \end{aligned} \quad (\text{S67})$$

where in the last line of (S66) and (S67), we applied the Feynman parameterization and $\not{y} \equiv y_\mu \gamma^\mu$ with $\mu \neq 1$. The Fourier transformation can be performed with the help of (S33),

$$\frac{-\not{y} - x\gamma^1}{(y^2 + \tilde{x}^2)} \rightarrow \frac{\pi^2}{4} \tilde{x}^{-1+\epsilon} i\not{k} - \frac{\pi^2}{4} \left(\tilde{x}^{-3+\epsilon} - \frac{q^2}{2} \tilde{x}^{-1+\epsilon} \right) x\gamma^1, \quad (\text{S68})$$

where $\not{k} = k_\mu \gamma^\mu$ for $\mu \neq 1$. We only list the terms that contribute to $\frac{1}{\epsilon}$ divergence, relevant to the one-loop RG calculations.

Now, we can use the result for the generalized function and then perform the integration in (S63). The contribution from $G_b D_b$ is

$$\begin{aligned} &\frac{\Gamma(\frac{d}{2})\Gamma(\frac{d-2}{2})}{8\pi^d} \int dx_1 dx_2 G(k, x, x_1) (-i\gamma^5) \left(\frac{\pi^2}{4} |x_1 - x_2|^{-1+\epsilon} i\not{k} - \frac{\pi^2}{4} |x_1 - x_2|^{-2+\epsilon} \text{sgn}(x_1 - x_2) \gamma^1 \right) (-i\gamma^5) \\ &\times G(k, x_2, 0) = -\frac{1}{16\pi^2\epsilon} \left[\frac{i\not{k}}{2q} - \frac{\gamma^1}{2} - \gamma^1 \left(\frac{i\not{k}}{2q} + \frac{\gamma^1}{2} \right) \right] e^{-qx}, \end{aligned} \quad (\text{S69})$$

the contribution from $G_s D_s$ is

$$\begin{aligned} & \frac{\Gamma\left(\frac{d}{2}\right)\Gamma\left(\frac{d-2}{2}\right)}{8\pi^d} \int dx_1 dx_2 G(k, x, x_1) (-i\gamma^5) \left(\gamma^1 \frac{\pi^2}{4} (x_1 + x_2)^{-2+\epsilon} \gamma^1 \right) (-i\gamma^5) G(k, x_2, 0), \\ & = \frac{1}{32\pi^2\epsilon} \left[\frac{i\mathbf{k}}{2q} - \frac{\gamma^1}{2} - \gamma^1 \left(\frac{i\mathbf{k}}{2q} + \frac{\gamma^1}{2} \right) \right] e^{-qx}, \end{aligned} \quad (\text{S70})$$

the contribution from $G_b D_s$ vanishes and the contribution from $G_s D_b$ is

$$\begin{aligned} & \frac{\Gamma(d-1)}{8\pi^d} \int_0^1 du u \int dx_1 dx_2 G(k, x, x_1) (-i\gamma^5) \left[\frac{\pi^2}{4} (x_1^2 + x_2^2 - 2(1-2u)x_1 x_2)^{-3/2+\epsilon/2} \gamma^1 (x_1 + x_2) \gamma^1 \right] (-i\gamma^5) \\ & \times G(k, x_2, 0) = \frac{1}{16\pi^2\epsilon} \left[\frac{i\mathbf{k}}{2q} - \frac{\gamma^1}{2} - \gamma^1 \left(\frac{i\mathbf{k}}{2q} + \frac{\gamma^1}{2} \right) \right] e^{-qx}. \end{aligned} \quad (\text{S71})$$

Hence, the total correction to the correlation function $\langle \psi \hat{\psi} \rangle$ reads

$$\langle \psi(k, x) \bar{\psi}(k', 0) \rangle = (2\pi)^{d-1} \delta(k - k') \left(1 - \frac{3g^2}{32\pi^2\epsilon} \right) \left[\frac{i\mathbf{k}}{2q} - \frac{\gamma^1}{2} - \gamma^1 \left(\frac{i\mathbf{k}}{2q} + \frac{\gamma^1}{2} \right) \right] e^{-qx}. \quad (\text{S72})$$

With the corrections in (S61) and (S72), the RG factors are

$$Z_{\partial\hat{\phi}} = 1 + \frac{\lambda}{16\pi^2\epsilon} + \frac{Ng^2}{4\pi^2\epsilon}, \quad Z_{\hat{\psi}} = 1 - \frac{g^2}{16\pi^2\epsilon}. \quad (\text{S73})$$

Accordingly, the corresponding anomalous dimensions are

$$\eta_{\partial\hat{\phi}} = \frac{1}{2} \frac{d \log Z_{\partial\hat{\phi}}}{d \log \mu} = -\frac{\lambda}{32\pi^2} - \frac{Ng^2}{8\pi^2}, \quad \eta_{\hat{\psi}} = \frac{1}{2} \frac{d \log Z_{\hat{\psi}}}{d \log \mu} = \frac{g^2}{32\pi^2}. \quad (\text{S74})$$

At the chiral Ising fixed point, we arrive at the results summarized in Table I.

B. Special transition

At the ordinary transition, the boson field obeys the Dirichlet boundary conditions. Hence, the boson propagator is (S39) with $w = 1$. The RG factors for the boundary fields are defined by [3],

$$\hat{\phi} = \sqrt{Z_\phi Z_{\hat{\phi}}^2} \hat{\phi}_R, \quad \hat{\phi}^2 = Z_{\hat{\phi}^2} \hat{\phi}_R^2, \quad \hat{\psi} = \sqrt{Z_\psi Z_{\hat{\psi}}^2} \hat{\psi}_R, \quad (\text{S75})$$

where $\hat{\phi}_R$, $\hat{\phi}_R^2$, and $\hat{\psi}_R$ denote the renormalized fields.

To obtain the scaling dimension for $\hat{\phi}$, we consider the correction to the correlation function $\langle \phi \hat{\phi} \rangle$. The one-loop Feynman diagram in Fig. 2 (a) gives,

$$\int dx_1 dx_2 D(p, x, x_1) G_2(p, x_1, x_2) D(p, x_2, 0). \quad (\text{S76})$$

Following a similar procedure employed in (S52)–(S61), and combining the result from the pure boson contribution [3], the divergence is

$$\langle \phi(p, z) \phi(p', 0) \rangle = (2\pi)^{d-1} \delta(p + p') \frac{e^{-pz}}{p} \left(1 + \frac{\lambda}{32\pi^2\epsilon} - \frac{3Ng^2}{8\pi^2\epsilon} \right). \quad (\text{S77})$$

Next, as discussed in the main text, the special transition has another relevant field, $\frac{1}{2}\hat{\phi}^2$. To this end, we consider the correction to the correlation function $\langle \phi \phi \frac{1}{2}\hat{\phi}^2 \rangle$. For the Feynman diagram shown in Fig. 2 (c), the contribution is identical to the fermion bubble correction to the boundary boson $\hat{\phi}$. Combining the correction from pure boson contribution [3], we arrive at

$$\langle \phi(p_1, x_1) \phi(p_2, x_2) \frac{1}{2} \hat{\phi}^2(P, 0) \rangle = (2\pi)^{d-1} \delta(P + p_1 + p_2) \frac{e^{-p_1 x_1 - p_2 x_2}}{p_1 p_2} \left(1 - \frac{\lambda}{16\pi^2\epsilon} - \frac{3Ng^2}{8\pi^2\epsilon} \right). \quad (\text{S78})$$

Finally, for the boundary fermion $\hat{\psi}$, the correction to the correlation function $\langle \psi \bar{\psi} \rangle$ is given, according to the one-loop Feynman diagram Fig. 2 (b), by

$$\int dx_1 dx_2 G(k, x, x_1) \tilde{G}_2(k, x_1, x_2) G(k, x_2, 0), \quad (\text{S79})$$

where $\tilde{G}_2(k, x_1, x_2) = \int d^{d-1} y e^{-ik \cdot y} (-i\gamma^5) G(y, x_1, x_2) (-i\gamma^5) D(y, x_1, x_2)$. The only difference is that the boson propagator satisfies the Neumann boundary condition. The calculation follows the previous discussion at the ordinary transition, and the final expression for the correction to the correlation function $\langle \psi \hat{\psi} \rangle$ reads,

$$\langle \psi(k, x) \bar{\psi}(k', 0) \rangle = (2\pi)^{d-1} \delta(k - k') \left(1 - \frac{5g^2}{32\pi^2\epsilon} \right) \left[\frac{ik}{2q} - \frac{\gamma^1}{2} - \gamma^1 \left(\frac{ik}{2q} + \frac{\gamma^1}{2} \right) \right] e^{-qx}. \quad (\text{S80})$$

With the corrections in (S77), (S78) and (S80), the RG factors are

$$Z_{\hat{\phi}} = 1 + \frac{\lambda}{16\pi^2\epsilon} - \frac{Ng^2}{4\pi^2\epsilon}, \quad Z_{\hat{\phi}^2} = 1 - \frac{\lambda}{16\pi^2\epsilon} - \frac{3Ng^2}{8\pi^2\epsilon}, \quad Z_{\hat{\psi}} = 1 - \frac{3g^2}{16\pi^2\epsilon}. \quad (\text{S81})$$

Accordingly, the corresponding anomalous dimensions are

$$\eta_{\hat{\phi}} = \frac{1}{2} \frac{d \log Z_{\hat{\phi}}}{d \log \mu} = -\frac{\lambda}{32\pi^2} + \frac{Ng^2}{8\pi^2}, \quad \eta_{\hat{\phi}^2} = \frac{d \log Z_{\hat{\phi}^2}}{d \log \mu} = \frac{\lambda}{16\pi^2} + \frac{Ng^2}{8\pi^2}, \quad \eta_{\hat{\psi}} = \frac{1}{2} \frac{d \log Z_{\hat{\psi}}}{d \log \mu} = \frac{3g^2}{32\pi^2}. \quad (\text{S82})$$

At the chiral Ising fixed point, we arrive at the results summarized in Table I.

IV. CHIRAL XY UNIVERSALITY CLASS

In this section, we calculate the boundary critical exponent for the chiral XY universality class. The chiral XY universality class can arise at the quantum phase transition between a Dirac semimetal and a Kekulé valence bond solid on a honeycomb lattice when the flavor of the Dirac fermion is large enough [45, 68]. The GNY action for the chiral XY universality class reads,

$$S = \int_{\mathcal{M}} d^d x \left(\sum_j \bar{\psi}_j \gamma^\mu \partial_\mu \psi_j + \frac{1}{2} \sum_{i=1,2} (\partial \phi_i)^2 + \frac{\lambda}{4!} \left(\sum_{i=1,2} \phi_i^2 \right)^2 + g \sum_j \left(\phi_1 \bar{\psi}_j \psi_j + i \phi_2 \bar{\psi}_j \gamma^5 \psi_j \right) \right). \quad (\text{S83})$$

In the absence of boundaries, the one-loop RG factor is well-known [65]:

$$Z_\phi = 1 - \frac{Ng^2}{4\pi^2\epsilon}, \quad Z_\psi = 1 - \frac{g^2}{8\pi^2\epsilon}, \quad (\text{S84})$$

$$Z_g = 1 + \frac{(1+N)g^2}{8\pi^2\epsilon}, \quad Z_\lambda = 1 + \frac{Ng^2}{2\pi^2\epsilon} + \frac{5\lambda}{24\pi^2\epsilon} - \frac{3Ng^4}{\lambda\pi^2\epsilon}. \quad (\text{S85})$$

Hence, the RG equation read

$$\frac{d\lambda}{d \log \mu} = -\epsilon\lambda + \frac{Ng^2\lambda}{2\pi^2} + \frac{5\lambda^2}{24\pi^2} - \frac{3Ng^4}{\pi^2}, \quad (\text{S86})$$

$$\frac{dg}{d \log \mu} = -\frac{\epsilon}{2}g + \frac{g^3}{8\pi^2} + \frac{Ng^3}{8\pi^2}. \quad (\text{S87})$$

It leads to the chiral XY fixed point at

$$\lambda^* = \frac{12\pi^2(1 - N + \sqrt{1 + 38N + N^2})}{5(1 + N)}\epsilon, \quad g^* = \frac{2\pi^2\sqrt{\epsilon}}{\sqrt{1 + N}}. \quad (\text{S88})$$

Consequently, the scaling dimensions for the boson and fermion are, respectively, given by

$$\Delta_\phi = 1 - \frac{1}{2 + 2N}\epsilon, \quad \Delta_\psi = \frac{3}{2} - \frac{1 + 2N}{4 + 4N}\epsilon. \quad (\text{S89})$$

Let's move on to the boundary criticality and take the Kekulé valence bond solid transition as an example. To be concrete, we consider a ribbon with two armchair boundaries. Recall that the two-component order parameter $\phi_{1,2}$ behaves as a “ \mathbb{Z}_3 ”

vector [45] under translation transformation. Now, because the translation symmetry is explicitly broken by the open boundaries, the boundary mass terms for ϕ_1 and ϕ_2 are no longer related. Moreover, it turns out that in the ribbon geometry, there is a mirror symmetry $x \rightarrow -x$ that can forbid the linear term for ϕ_2 , but in general, a linear term in ϕ_1 is allowed on the boundary. Hence, the boundary boson ϕ_1 will obey a normal boundary condition due to the presence of a linear term, while the boundary boson ϕ_2 can still satisfy distinct boundary conditions determined by the mass term. The normal boundary condition in the GNY universality class is still an outstanding question, and we leave the investigation to a future work. In the following, we assume that the linear term in ϕ_1 is absent, and consider independent boundary conditions for the two components $\phi_{1,2}$, respectively.

Due to the lack of symmetry relation on the boundary, the boson boundary conditions can be classified into four cases:

1. Both ϕ_1 and ϕ_2 satisfy the Neumann boundary condition.
2. Both ϕ_1 and ϕ_2 satisfy the Dirichlet boundary condition.
3. ϕ_1 satisfies the Neumann boundary condition while ϕ_2 satisfies the Dirichlet boundary condition.
4. ϕ_1 satisfies the Dirichlet boundary condition while ϕ_2 satisfies the Neumann boundary condition.

In most cases, the calculations follow the same procedures as for the chiral Ising universality class. However, due to the lack of a symmetry operation that forbids the ϕ_1 component, as detailed in the previous paragraph and in the main text, it gives rise to an additional Feynman diagram, shown in Fig. 2 (d), to boundary fermion correction. This Feynman diagram leads to the following contribution to the correlation function $\langle \psi \hat{\psi} \rangle$,

$$\int dx_1 dx_2 G(k, x, x_1) \mathbb{I}G(k, x_1, 0) D(k', x_1, x_2) (-\text{Tr} [\mathbb{I}G(y = 0, x_2, x_2)]), \quad (\text{S90})$$

$$\begin{aligned} &= \int dx_1 dx_2 G(k, x, x_1) G(k, x_1, 0) D(k', x_1, x_1) \times \left(-\frac{x_2^{-3+\epsilon}}{4\pi^2\epsilon} \right) \\ &= \frac{1}{8\pi^2\epsilon} \left[\frac{i\mathbf{k}}{2q} - \frac{\gamma^1}{2} - \gamma^1 \left(\frac{i\mathbf{k}}{2q} + \frac{\gamma^1}{2} \right) \right] e^{-qx}. \end{aligned} \quad (\text{S91})$$

Incorporating this difference, the final results at the one-loop order are summarized below.

1. Both ϕ_1 and ϕ_2 satisfy the Neumann boundary condition:

$$\begin{aligned} \Delta_{\hat{\psi}} &= \frac{3}{2} - \frac{1+2N}{2+2N}\epsilon, \\ \Delta_{\hat{\phi}_1} &= 1 - \frac{6+9N+\sqrt{1+38N+N^2}}{10+10N}\epsilon, \\ \Delta_{\hat{\phi}_2} &= 1 - \frac{6-N+\sqrt{1+38N+N^2}}{10+10N}\epsilon, \\ \Delta_{\hat{\phi}_1^2} &= 2 - \frac{8+7N-2\sqrt{1+38N+N^2}}{10+10N}\epsilon, \\ \Delta_{\hat{\phi}_2^2} &= 2 - \frac{8-3N-2\sqrt{1+38N+N^2}}{10+10N}\epsilon. \end{aligned}$$

2. Both ϕ_1 and ϕ_2 satisfy the Dirichlet boundary condition:

$$\Delta_{\hat{\psi}} = \frac{3}{2} - \frac{2N+1}{2+2N}\epsilon, \quad (\text{S92})$$

$$\Delta_{\partial\hat{\phi}_1} = 2 - \frac{6-N+\sqrt{1+38N+N^2}}{10+10N}\epsilon, \quad (\text{S93})$$

$$\Delta_{\partial\hat{\phi}_2} = 2 - \frac{6+9N+\sqrt{1+38N+N^2}}{10+10N}\epsilon. \quad (\text{S94})$$

3. ϕ_1 satisfies the Neumann boundary condition while ϕ_2 satisfies the Dirichlet boundary condition:

$$\begin{aligned}\Delta_{\hat{\psi}} &= \frac{3}{2} - \frac{3+4N}{4+4N}\epsilon, \\ \Delta_{\hat{\phi}_1} &= 1 - \frac{6+9N+\sqrt{1+38N+N^2}}{10+10N}\epsilon, \\ \Delta_{\hat{\phi}_1^2} &= 2 - \frac{8+7N-2\sqrt{1+38N+N^2}}{10+10N}\epsilon, \\ \Delta_{\partial\hat{\phi}_2} &= 2 - \frac{6+9N+\sqrt{1+38N+N^2}}{10+10N}\epsilon.\end{aligned}$$

4. ϕ_1 satisfies the Dirichlet boundary condition while ϕ_2 satisfies the Neumann boundary condition:

$$\begin{aligned}\Delta_{\hat{\psi}} &= \frac{3}{2} - \frac{1+4N}{4+4N}\epsilon, \\ \Delta_{\partial\hat{\phi}_1} &= 2 - \frac{6-N+\sqrt{1+38N+N^2}}{10+10N}\epsilon, \\ \Delta_{\hat{\phi}_2} &= 1 - \frac{6-N+\sqrt{1+38N+N^2}}{10+10N}\epsilon, \\ \Delta_{\hat{\phi}_2^2} &= 2 - \frac{8-3N-2\sqrt{1+38N+N^2}}{10+10N}\epsilon.\end{aligned}$$